Dalton Transactions

PAPER

Cite this: *Dalton Trans.*, 2016, **45**, 10050

Ca(II) and Ce(III) homogeneous alginate hydrogels from the parent alginic acid precursor: a structural study

Juan Manuel Sonego,[a] Patricio R. Santagapita,[b] Mercedes Perullini*[a] and Matías Jobbágy*[a]

Received 22nd January 2016,
Accepted 30th March 2016

DOI: 10.1039/c6dt00321d

www.rsc.org/dalton

Alginate hydrogels are suitable for the encapsulation of biomolecules and microorganisms for the building of bioactive materials. Several alternatives to the conventional alginate formulation are being studied for a broad range of biotechnological applications; among them the crosslinking of alginate by lanthanide cations, Ln(III), envisages expanded biomedical applications. The performance of these functional materials is highly related to the microstructure of the alginate matrix, which in turn is affected by the conditions of synthesis. In particular, when a diffusing gradient of the crosslinking cation is involved, microstructure inhomogeneities are expected at the macroscopic level. Here we discuss the subtle differences in the microstructure, as assessed by SAXS (Small Angle X-ray Scattering), established in the direction of the gradient of diffusion of Ca(II) or Ce(III).

Introduction

Natural polymer based hydrogels play a key role in the development of advanced biomaterials, ranging from scaffolds[1] to cell loaded artificial organs as well as biodegradable drug delivery platforms.[2,3] Among them, the alginate based ones demonstrated wide acceptance due to their inherent biocompatibility and versatility.[4–7] This biopolymer consists of linear copolymers that contain monomers of (1,4)-linked β-D-mannuronic acid (M) and its C-5 epimer, α-L-guluronic acid (G) residues. These units are covalently linked together in different sequences or blocks composed by the same unit (MMMMM or GGGGGG) or alternating them (GMGMGM); the relative amount of each monomer and the spatial distribution is ruled by the nature of the alginate source.[8] Typically, hydrogels are prepared by subjecting a soluble Na(I)–alginate solution to crosslink its chains by M(II) complexation, giving rise to M(II)–Alg hydrogels. Among cations, Ca(II) is preferred due to its intrinsic biocompatibility. Alginates can also form hydrogels once soluble Na(I)–alginate chains are significantly protonated in moderate acidic media (pH 4.5).[9]

However, transition metal cations and trivalent lanthanides, Ln(III), can easily drive this process.[10–14] An interesting cation due to its redox and antimicrobial properties is Ce(III),[15] alginate hydrogels of which have not been sufficiently studied so far. Cerium oxide nanoparticles commonly known as nanoceria are efficient free radical scavengers and are considered as a potent therapeutic option for many biomedical applications.[16,17] However, opposed to their beneficial effects, the cytotoxicity induced by nanoparticles themselves undermines the potential of nanoceria in therapeutics. Thus, the couple Ce(III)/Ce(IV) embedded in an intrinsic biocompatible alginate matrix, could offer a safer platform for future applications.

During the last few decades, the microstructure of alginate hydrogels has been extensively studied mainly by Small Angle X-Ray Scattering (SAXS). It has been shown that the alginate backbone in the hydrogel is dependent on the composition (M/G ratio) and concentration of Na(I)–alginate as well as on the employed crosslinking cation.[18,19] In particular, for Ca(II)–Alg hydrogels SAXS patterns are indicative of rod like objects randomly orientated, while for alginic acid samples the formation of junction zones with a high degree of multiplicity was suggested.[20]

It is known that certain properties of ionotropic alginate hydrogels are affected by the crosslinking procedure.[21] One of the methods more extensively used in the synthesis of alginate hydrogels as an immobilization matrix is the diffusional setting (by which beads, fibers or films can easily be obtained) and where the crosslinking cations diffuse through a solution of sodium alginate.[4] This method generates inhomogeneous

[a]*INQUIMAE-DQIAyQF, Universidad de Buenos Aires, Ciudad Universitaria, Pab. II, C1428EHA, Buenos Aires, CONICET, Argentina. E-mail: mercedesp@qi.fcen.uba.ar, jobbag@qi.fcen.uba.ar*

[b]*Departamento de Industrias-DQO, Facultad de Ciencias Exactas y Naturales, Universidad de Buenos Aires, Ciudad Universitaria, Pab. II, C1428EHA, Buenos Aires, CONICET, Argentina*

materials due to the cation diffusion gradient established from the non-gelled center toward the boundaries.[22,23] Furthermore, the formation of parallelly aligned capillary structures has been demonstrated in alginates obtained by the external addition of the crosslinking cation, which affect the functional behavior of the material.[24] The homogeneous generation or release of crosslinking cations is difficult to achieve. In contrast, hydrogels prepared from alginic acid reach a more stable structure that depends to a lesser extent on the preparation method.[25] One particular procedure based on the *in situ* homogeneous release of protons resulting from the hydrolysis of D-glucono-δ-lactone (GDL) allows a gradient-free gelation from the soluble Na(I) to the insoluble H(I) one. The pH descends to a mild value of acidity, inherently fixed by the alginate/alginic acid buffer at around pH 4.5, as well as the mild temperatures required for GDL's hydrolysis guarantee the preservation of alginate chains' integrity.[26]

The objective of this work is to determine whether the uniform microstructure obtained from homogeneous gelation with GDL can be preserved when replacing the H^+ by different metallic cations in order to overcome the inhomogeneities that arise from ionotropic diffusing methods. On the other hand, we intend to characterize the microstructure of Ce(III)–alginate hydrogels as a representative example of Ln(III)–alginate hydrogels. These hydrogels constitute promissory matrices for the development of novel functional biomaterials.[27]

Materials and methods

Synthesis of alginate hydrogel samples

Alginic acid sodium salt from brown algae (bioreagent grade), D-(+)-gluconic acid δ-lactone (99–100%), calcium chloride dihydrate ($CaCl_2{\cdot}2H_2O$, 99%) and cerium(III) chloride heptahydrate ($CeCl_3{\cdot}7H_2O$, 99.9%) were purchased from Sigma-Aldrich. All samples were prepared using solutions of alginic acid sodium salt from brown algae (Na–alg) with a concentration of 1.0% or 2.0% in weight. Samples are labeled "1" or "2" depending on the Na–alg concentration employed.

Unlike the most common method for the preparation of alginate hydrogels (*i.e.* by dropwise addition of Na–alg solutions into the gelling media), in this work we poured the Na–alg solution into acrylic molds and allowed the diffusion of the gelling agent through a dialysis membrane (Medicell® International Ltd, code DTV.12000.09, molecular weight cut-off 14 000 Daltons), satisfying the boundary conditions for the one-dimension diffusion of the crosslinking cation. Samples are labeled "Ca" or "Ce" when 0.10 M $CaCl_2$ or, 0.10 M $CeCl_3$, respectively, is used as a crosslinking solution.

Gelation of the acidic alginate series (samples "H") was achieved by homogeneous acidification with 0.20 mM gluconic acid δ-lactone (GDL). After a 24 h crosslinking time, some of these samples cast into acrylic molds were allowed to interchange H^+ by Ca(II) and/or Ce(III) using the same strategy described above. This series of samples are labeled "H/Ca", "H/Ce" and "H/CaCe" when 0.10 M $CaCl_2$, 0.10 M $CeCl_3$ or 0.05 M $CaCl_2$/0.05 M $CeCl_3$, respectively, is used as the exchange solution.

In all cases, when a crosslinking or interchanging $CaCl_2$ or $CeCl_3$ solution is employed, the concentration of the solution in contact with the sample is kept constant for 7 days, after which the system is considered to have reached equilibrium.

Transport properties

Water self-diffusion coefficients (D) within hydrogel samples were obtained at 25 °C by Low-field proton Nuclear Magnetic Resonance (LF-^{1}H-NMR) measurements using a Bruker Minispec mq20 spectrometer (Bruker BioSpin GmbH, Rheinstetten, Germany) with a 0.47 T magnetic field operating at a resonance frequency of 20 MHz. All samples were previously equilibrated at 25.00 ± 0.01 °C in a thermal bath (Haake, model Phoenix II C35P, Thermo Electron Corporation Gmbh, Karlsruhe, Germany). D measurements were performed through the pulsed magnetic field gradient spin echo (PGSE) sequence,[29] in which two controlled magnetic field gradients are applied in a spin echo pulse sequence between 90° and 180° pulses, and between the 180° pulse and the acquisition, respectively. The applied magnetic field gradient intensity (G) was calibrated in the range between 1.4 and 2.5 T m^{-1} (R^2 = 0.999911) by employing a 1.25 g L^{-1} $CuSO_4{\cdot}5H_2O$ water solution, characterized by a known D value of $(2.29 \pm 0.01) \times 10^{-9}$ m^2 s^{-1} at 25 °C.[28]

Samples were considered as characterized by a single self-diffusion coefficient; then, D could be measured by registering the amplitude (A) of the PGSE signal with ($A_{G(t)}$) and without ($A_{G(0)}$) an applied field gradient (G), according to eqn (I):

$$\ln\frac{A_{(G(t))}}{A_{(G(0))}} = \gamma^2 D\delta^2\left(\Delta - \frac{1}{3}\delta\right)G^2 \quad \text{(I)}$$

where δ is the gradients length, Δ is the time between the gradients, and γ is the proton gyromagnetic ratio. The samples were analyzed by setting the magnetic field gradient amplitude to 2 T m^{-1}, τ (the time between 90° and 180° pulses) to 7.5 ms, δ to 0.5 ms, and Δ to 7.5 ms. The number of scans, the recycle delay and gain were 16, 2 s and 66 dB, respectively.[29]

In all cases, the measurements were made in duplicate on three independent hydrogel samples. The effect of crosslinking or interchanging $CaCl_2$ and/or $CeCl_3$ solutions on D was analyzed by 1 way ANOVA with the Tukey post test using Prism 5 (GraphPad Software Inc., San Diego, CA, USA).

SAXS characterization of the microstructure

The microstructure characterization was performed at the LNLS SAXS2 beamline in Campinas, Brazil, working at λ = 0.1488 nm, wave vector range: 0.08 nm^{-1} < q < 1.6 nm^{-1}. All the alginate hydrogel samples showed isotropic scattering and were modeled as a fractal system composed of rod-like structures, although the rigorous interpretation of experimental results as indicating "fractality" requires many orders of magnitude of power-law scaling.[30,31] The structure of the hydrogel

samples is characterized by three parameters: the rod cross-sectional radius (R), the fractal dimension at distances higher than R (α_1) describing the multiplicity of the junction zone, and the fractal dimension at distances lower than R (α_2) describing the degree of compactness within the rods.

Parameters α_1 and α_2 were evaluated from the slope of the scattering intensity averaged along azimuthal angles *versus* the scattering vector q in the log–log scale at low and high values of q, respectively. The radius of gyration of the rods was obtained from the q value corresponding to the intersection of both power law regions. The Kratky plot: scattering intensity multiplied by the square modulus of the scattering vector, $I(q)\cdot q^2$, as a function of the modulus of the scattering vector, q, gives a maximum value at the intersection of power law regions and allows the calculation of parameter R. The scattering behavior of a collection of randomly oriented rods should exhibit a maximum for such a plot at $q \approx 1/R_g$, R_g being the mean gyration radius in the cross-section of the rods. The outer radius of the fibrils (parameter R) is then given by $R = R_g\sqrt{2}$.

Hydrogel samples were cast in 1.00 cm thick acrylic molds and previous to SAXS determinations, three slices were taken at different distances from the cation solution boundary (0.00–0.05 mm, 0.05–0.10 mm and 0.10–0.15 mm). In all cases, the measurements were made in triplicate on each of the slices obtained from two independent hydrogel samples.

Results

Fig. 1 shows the water self-diffusion coefficient values (D) of hydrogel samples obtained by LF-NMR. For gels or diluted polysaccharide systems, the general response obtained by NMR will be given by water protons modulated by the exchange between them and the protons of the biopolymers.[32,33] Then, a decrease of the overall mobility is expected. The magnitude of this decrease depends on the reduced flexibility of the biopolymer chains with respect to water, the aggregation state and on whether the systems are gelled or not. As expected, all alginate gels showed reduced D values in comparison with water, $(2.30 \pm 0.01) \times 10^{-9}$ m^2 s^{-1}. Ionotropic gels obtained by crosslinking solutions of Ca(II) or Ce(III) present a similar value of D ($\sim 2.15 \times 10^{-9}$ m^2 s^{-1}) with no significant differences between the crosslinking cation or the alginate concentration. However, especially for Ce(III), on increasing the alginate concentration, a slight tendency towards lower D values is observed. The closer framework obtained with a higher concentration of the biopolymer is expected to cause a slower diffusion within the aqueous pores, however given the gelation and concentrations of alginate used in this study, this effect must be extremely small.[34]

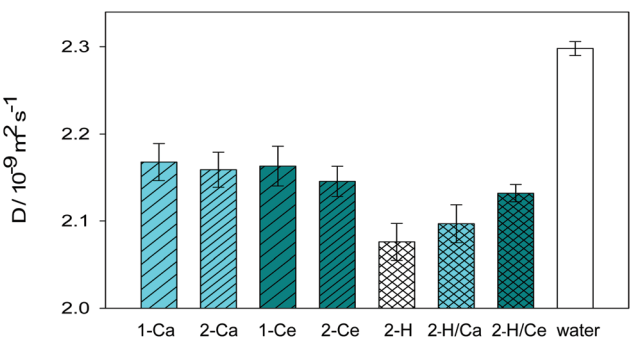

Fig. 1 LF-NMR obtained water self-diffusion coefficient values (D) of hydrogels generated by sodium alginate 1 wt% or 2 wt% ("1" or "2") crosslinking with $CaCl_2$ ("Ca") or $CeCl_3$ ("Ce") solutions, alginic acid hydrogel ("H"), and hydrogels obtained by the cation exchange of an alginic acid sample with $CaCl_2$ or $CeCl_3$ solutions ("H/Ca" and "H/Ce", respectively).

In the case of alginic acid gel (H–alg) only a higher concentration (*i.e.* 2% in weight) of the Na–alg solution generated a self-supporting hydrogel, and thus no considerations with respect to the biopolymer concentration effect can be made. Nonetheless, the alginic acid gel structure gives a significantly lower value of D, $(2.07 \pm 0.02) \times 10^{-9}$ m^2 s^{-1}, as compared to samples obtained from the same sodium alginate concentration crosslinked with Ca(II) or Ce(III), $(2.16 \pm 0.02) \times 10^{-9}$ m^2 s^{-1} and $(2.14 \pm 0.02) \times 10^{-9}$ m^2 s^{-1} respectively, which is in good agreement with a higher degree of interconnectivity of rods in the microstructure as previously observed in the acidic gelation.[20]

Interestingly, when the Ca(II) or Ce(III)–alginate structure is obtained after cation exchange from the alginic acid gel, in the case of Ce(III) the water diffusion value is similar to that of the original ionotropic gel, while for Ca(II) the value of D is significantly lower. This suggests that there is a memory effect in the sample microstructure; the Ca(II)–alginate sample obtained by cation exchange is somehow similar to the parent alginic hydrogel sample. It is worth noting that the water self-diffusion coefficient value of samples 2H and 2-H/Ca presents no significant differences, while the value of D is higher for the Ce(III) exchanged sample (*i.e.* 2-H/Ce). One possible explanation could reside in the higher coordination number of lanthanide ions resulting in a malleable accommodation of the carboxylate groups of alginate chains, giving as a result a more flexible framework.

The structure of the hydrogel samples was investigated by Small Angle X-ray Scattering (SAXS) analysis. As for previous studies, ionotropic alginate and alginic acid gels showed isotropic scattering and were modeled as a fractal system composed of rod-like structures. Their structure was characterized by three parameters: the rod cross-sectional radius (R), the fractal dimension at distances higher than R (α_1) describing the multiplicity of the junction zone, and the fractal dimension at distances lower than R (α_2) describing the nanostructure within the rods. Fig. 2 shows a typical SAXS scattering profile, indicating the power law regimes at a low and high q and the Kratky plot, which gives a maximum value at the intersection of power law regions and allows the calculation of parameter R.

The characteristic log–log SAXS profiles exhibit an asymptotic behavior at low q-values (in the experimental q range

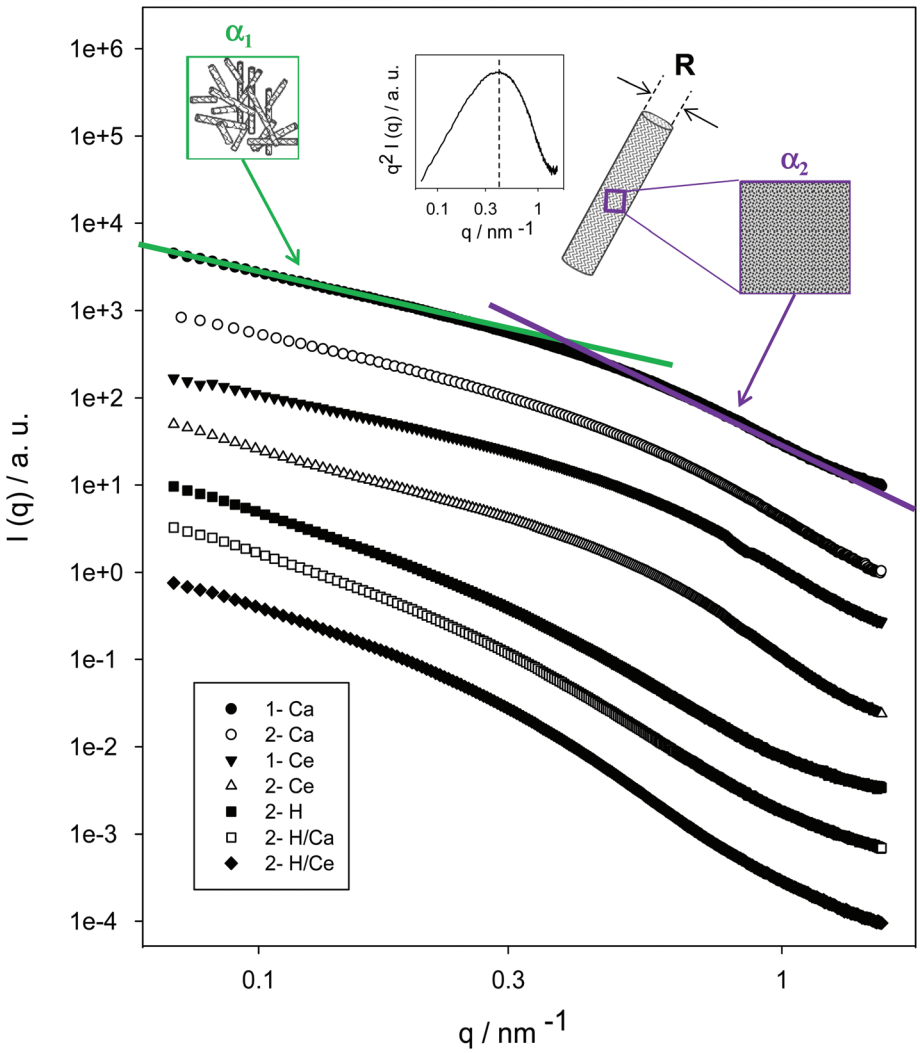

Fig. 2 log–log SAXS profile plots of representative samples of hydrogels generated by sodium alginate 1 wt% or 2 wt% ("1" or "2") crosslinking with $CaCl_2$ ("Ca") or $CeCl_3$ ("Ce") solutions, alginic acid hydrogel ("H"), and hydrogels obtained by the cation exchange of an alginic acid sample with $CaCl_2$ or $CeCl_3$ solutions ("H/Ca" and "H/Ce"). Parameters α_1 and α_2 were evaluated from the slope of the scattering intensity at low and high values of q, respectively, and the radius of gyration of the rods (parameter R) was obtained from the Kratky plot (inset).

0.09 to 0.3 nm^{-1}), close to $I(q) \approx q^{-\alpha_1}$. The parameter α_1 reflects the degree of interconnection of the rods composing the structure. As shown in Fig. 3, while Ca(II)–alginate gels present values of α_1 close to 1 (assignable to randomly oriented rods), H(I)–alginate samples show values of α_1 close to 2 (interconnected rods). Ce(III)–alginate samples exhibit slightly higher values of α_1 than those for Ca(II)–alginates, suggesting that the trivalent lanthanide cation could favor a more interconnected structure *via* the coordination of carboxylic groups belonging to more than two alginate chains, as the egg-box model predicts.[35]

Another inherent difference arises with respect to the homogeneity of the microstructure, since in conventional ionotropic alginates, hydrogels are obtained by slow diffusion of the gelling agent (Ca(II) or Ce(III)). In order to evaluate this effect, and as described in the Materials and methods section, the diffusion of the gelling agent was allowed through a dialysis membrane, satisfying the boundary conditions for one-dimension diffusion. Once totally gelled (24 h), SAXS experiments were performed on 0.5 mm thick slices of each hydrogel sample, taken at different distances in the direction perpendicular to the dialysis membrane, collecting representative portions along the former gelation gradient. As shown in Fig. 3, the parameter α_1 increases as a function of the distance to the interface for Ca(II)–alginate samples, showing a moderate increase for 1.0 wt% alginate concentration and a more marked increase in the case of 2 wt% alginate concentration. The concentration of free Ca(II) is 0.1 M in the immediacy of the dialysis membrane and decreases abruptly in the alginate gel with the distance from the boundary of the crosslinking cation supply. The variation of α_1 with the ratio of Ca(II)/alginate concentration can be interpreted in the frame of the egg-box model[35] proposed to describe the interaction of alginate chains with divalent cations. When the concentration of Ca(II)

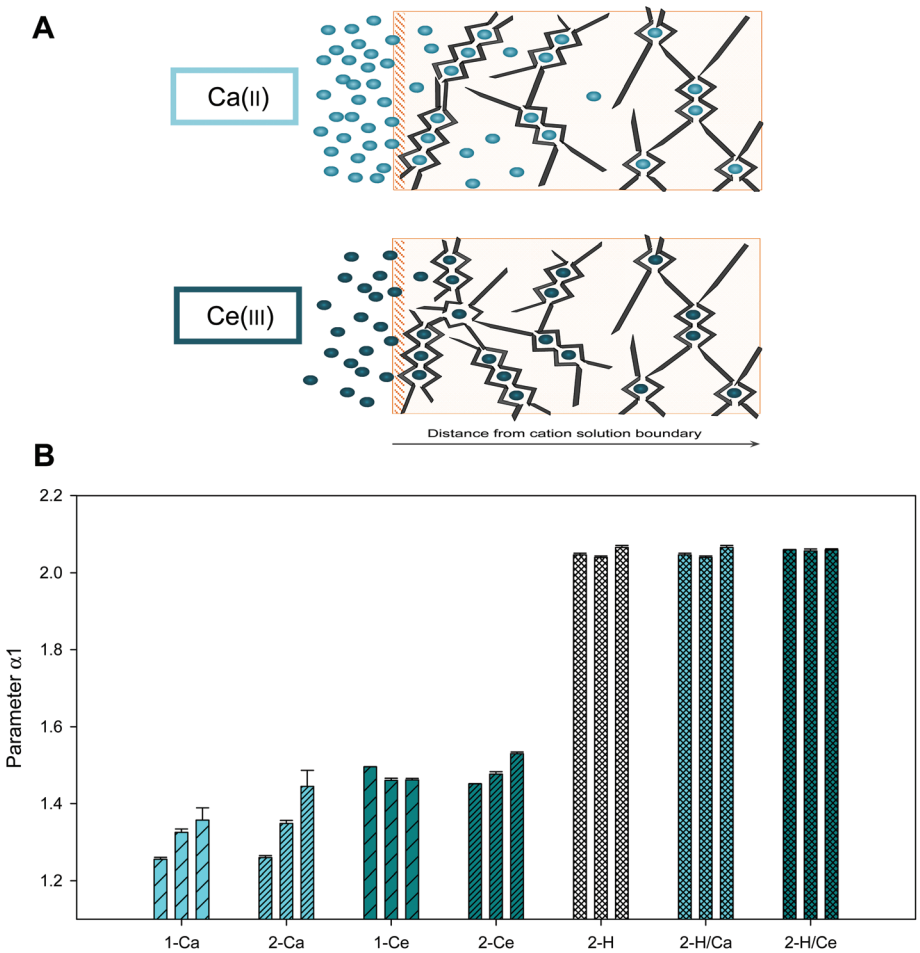

Fig. 3 (A) Schematic representation of gelation. For a high concentration of Ca(II) (*i.e.* near the cation solution boundary), progressive and cooperative fixation of the crosslinking cation favors dimerization of alginate chains while for a low concentration of Ca(II), the random binding of Ca(II) promotes inter-chain crosslinking, giving as a result a higher degree of connectivity of rods (*i.e.* higher value of parameter α_1). In the case of Ce(III), a high degree of inter-chain crosslinking is possible even at a high concentration of the cation due to the formation of tripartite junction nodes. (B) Parameter α_1 of the microstructure derived from log–log SAXS profiles. Three values from each sample are presented, corresponding to slices of the hydrogel taken at different distances from the cation solution boundary (from left to right: 0.00–0.05 mm, 0.05–0.10 mm and 0.10–0.15 mm). Samples correspond to sodium alginate 1 wt% or 2 wt% ("1" or "2") crosslinked with $CaCl_2$ or $CeCl_3$ solutions ("Ca" and "Ce", respectively), alginic acid hydrogel ("H"), and hydrogels obtained by the cation exchange of an alginic acid sample with $CaCl_2$ or $CeCl_3$ solutions ("H/Ca" and "H/Ce", respectively).

is in the order of guluronate stoichiometry, dimerization of alginate chains involving the site binding of Ca(II) cations to interior faces of the chains in a sandwich-like geometry is expected to occur with a low degree of multiple chain interconnections, while for a low concentration of the divalent cation, randomly spaced Ca(II) could bind and coordinate different alginate chains (see the schematic representation of gelation in Fig. 3).

Compared with Ca(II), Ln(III) cations offer a more versatile and larger coordination environment, expanding the possible chain arrays within the crosslinked hydrogel, resulting in more ramified networks.[36] So, the higher value observed for α_1 in the case of Ce(III)–alginate hydrogels in comparison with Ca(II)–alginate systems can be directly explained from these events of the coordination of carboxylic groups from three different alginate chains. However, the incidence of these "tripartite junction nodes" is highly dependent on the alginate concentration, which is not constant throughout the final gelled structure due to the slow diffusion of the polymer chains toward the reaction front. From these opposing effects it can be seen that the value of α_1 remains approximately constant with the distance to the reaction front and presents higher values with respect to Ca(II)–alginate. It is worth mentioning that the effect of the polymer concentration gradient seems to be less noticeable for systems with a high concentration of alginate (2 wt%), as a slight increase in α_1 with the distance to the reaction front is evidenced.

As mentioned above, H(I)–alginate samples present values of α_1 close to 2, reflecting a more interconnected structure. These results are in good agreement with previously reported data[20] and support the water self-diffusion coefficient values presented previously (see Fig. 1). Hydrogels prepared from

alginic acid with the *in situ* homogeneous release of protons resulting from the hydrolysis of D-glucono-δ-lactone (GDL) ensure a gradient-free gelation from the soluble Na(I) to the insoluble H(I) one. The homogeneity in the hydrogel microstructure was corroborated from SAXS experiments as no fluctuations of the parameter α_1 were observed throughout the assessment of different portions. Interestingly, the samples obtained from this phase by further cation (Ca(II) or Ce(III)) exchange maintain the multiple junction morphology of the parent H–alginate hydrogels and the homogeneous nature of the microstructure (*i.e.* no effect from cation diffusion gradient is observed). This has a very important implication since a cation crosslinked alginate hydrogel with a multiple junction instead of a nanofibrillar morphology can be easily obtained. Furthermore, following this simple procedure a homogeneous microstructure can be achieved independent of cation concentration gradients.

The characteristic size of the rods composing the structure is deduced from the maxima observed on Kratky plots. As shown in Fig. 4A, the value obtained for the H(I)–alginate system was $R = (14.9 \pm 0.2)$ nm while ionotropic gels presented much lower values $R \approx 4$ nm, in agreement with previous observations.[20] In line with the results obtained for parameter α_1, when the Ca(II) or Ce(III)–alginate structure is obtained after cation exchange from the alginic acid gel, the radius of gyration of the rods that is typical of the parent H(I)–alginate hydrogels is maintained ($R = 15.8 \pm 0.2$ nm and 14.6 ± 0.8 nm for Ca(II) and Ce(III)–alginate, respectively). Both, the degree of interconnection (parameter α_1) and the size of the rods composing the structure (parameter R) reinforce the hypothesis of a memory effect in the sample microstructure made when analyzing the water self-diffusion coefficient values (D).

On the other hand, for the totality of samples the parameter α_2 denoting the compactness of the nanostructure of hydrogels (*i.e.*, secondary structure) takes values from 3.0 to 4.2 (see Fig. 4B). For ionotropic gels, we observed the same trend for a low and high alginate content: Ce(III)-crosslinked structures exhibited a higher value of α_2 (3.6 *versus* 3.0 and 4.0 *versus* 3.4 for 1 wt% and 2 wt% alginate, respectively). When an equimolar mixture of both cations was used as a crosslinking solution, the resulting hydrogel showed a degree of compactness of the nanostructure intermediate to the crosslinking with individual cations (low alginate concentration) or similar to Ce(III) crosslinking (high alginate concentration). The alginic acid gel presented a value of α_2 in the same range (3.5) and the cationic alginates derived from it presented values somewhat higher (α_2 = 3.6, 4.2 and 4.0 nm for Ca(II)–, Ce(III)– and Ca(II)/Ce(III)–alginate, respectively). This goes on to show that although the microstructure of rods is inherited for the parent morphology (reflected in parameter R), the nanostructure within the rods is consistent with the type of cation exchanged, presenting a similar degree of compactness as the original ionotropic alginate (reflected in parameter α_2). The mean gyration radius in the cross-section of the rods (R) and the compactness of the rod structure at the nanoscale (α_2) are not dependent on the distance to the reaction front and thus the results in Fig. 4 are presented as an average of all the six samples taken at different distances from the diffusional front.

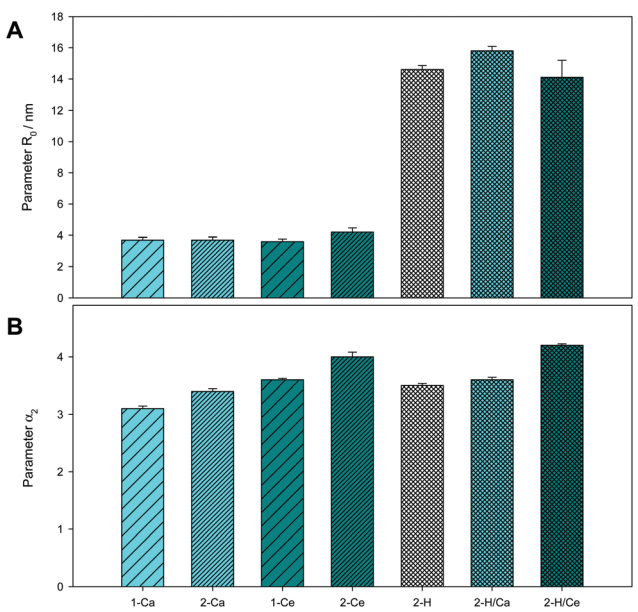

Fig. 4 (A) Parameter R assimilable into the outer radius of the fibrils (nm) deduced from the maxima observed on Kratky plots (see Fig. 2B). (B) Parameter α_2 derived from log–log SAXS profiles in the q range 0.6–1.0 nm^{-1}. Samples correspond to sodium alginate 1 wt% or 2 wt% ("1" or "2") crosslinked with $CaCl_2$ or $CeCl_3$ solutions ("Ca" and "Ce", respectively), alginic acid hydrogel ("H"), and hydrogels obtained by the cation exchange of an alginic acid sample with $CaCl_2$ or $CeCl_3$ solutions ("H/Ca" and "H/Ce", respectively).

Conclusions

Here we show that in conventional ionotropic alginate hydrogels, the cation gradient effect generates gradual changes in the microstructure with respect to the degree of interconnection of the rods composing the structure (parameter α_1). However, the mean gyration radius in the cross-section of the rods (parameter R) and the compactness of the rod structure at the nanoscale (α_2) are not dependent on the distance to the reaction front, showing constancy within the sample.

It has been demonstrated that the Ca(II) and Ce(III)–alginate samples obtained by cation exchange from the homogeneous H–alginate hydrogel maintain the multiple junction structural pattern as well as the homogeneous nature of the microstructure from the parent hydrogel (*i.e.* no effect from cation diffusion gradient is observed). This has a very important implication since following this simple procedure a homogeneous microstructure can be achieved, in contrast to the inhomogeneous materials obtained by conventional procedures constrained by cation concentration gradients and alginate chain migration towards the gelling front.

A detailed study of the structure as revealed from SAXS analysis shows that although the microstructure of the rods is

inherited for the parent morphology (reflected in parameter R), the nanostructure within the rods is consistent with the type of cation exchanged, presenting a similar degree of compactness as the original ionotropic alginate (reflected in parameter α_2). Thus, a cation crosslinked alginate matrix exhibiting multiple junctions instead of a nanofibrillar morphology can be easily obtained. This fine control is expected to affect relevant parameters such as sorption, exchange and transport kinetics, as well as inherent dissolution kinetics and size exclusion of the obtained hydrogels. These physicochemical parameters define the performance of these phases in most of the present and potential biomedical and environmental applications.

Acknowledgements

This work was supported by the Brazilian Synchrotron Light Laboratory (LNLS, Brazil, proposals SAXS1-14280 and D11A-SAXS-6039), University of Buenos Aires (UBACyT 20020130100610BA), Agencia Nacional de Promoción Científica y Tecnológica (ANPCyT PICT 2013 2045, 2013 0434 and 2012 1167) and Consejo Nacional de Investigaciones Científicas y Técnicas (CONICET PIP 11220110101020). JMS acknowledges CONICET for a postdoctoral fellowship. MP, PRS and MJ are Research Scientists of CONICET (Argentina).

References

1 J. L. Drury and D. J. Mooney, Hydrogels for tissue engineering: scaffold design variables and applications, *Biomaterials*, 2003, **24**(24), 4337–4351.
2 A. S. Hoffman, Hydrogels for biomedical applications, *Adv. Drug Delivery Rev.*, 2012, **64**(Supplement), 18–23.
3 W. R. Gombotz and S. F. Wee, Protein release from alginate matrices, *Adv. Drug Delivery Rev.*, 1998, **31**(3), 267–285.
4 O. Smidsrod and G. Skjakbraek, Alginate as Immobilization Matrix for Cells, *Trends Biotechnol.*, 1990, **8**(3), 71–78.
5 J. A. Rowley, G. Madlambayan and D. J. Mooney, Alginate hydrogels as synthetic extracellular matrix materials, *Biomaterials*, 1999, **20**(1), 45–53.
6 M. Perullini, *et al.*, Alginate/porous silica matrices for the encapsulation of living organisms: tunable properties for biosensors, modular bioreactors, and bioremediation devices, *Mesoporous Biomater.*, 2015, **2**, 3–12.
7 M. Perullini, *et al.*, Improving bacteria viability in metal oxide hosts via an alginate-based hybrid approach, *J. Mater. Chem.*, 2011, **21**(12), 8026–8031.
8 A. D. Augst, H. J. Kong and D. J. Mooney, Alginate hydrogels as biomaterials, *Macromol. Biosci.*, 2006, **6**(8), 623–633.
9 C. Spedalieri, *et al.*, Silica@proton-alginate microreactors: A versatile platform for cell encapsulation, *J. Mater. Chem. B*, 2015, **3**(16), 3189–3194.
10 R. Brayner, *et al.*, Alginate-Mediated Growth of Co, Ni, and CoNi Nanoparticles: Influence of the Biopolymer Structure, *Chem. Mater.*, 2007, **19**(5), 1190–1198.
11 P. Agulhon, *et al.*, Controlled synthesis from alginate gels of cobalt–manganese mixed oxide nanocrystals with peculiar magnetic properties, *Catal. Today*, 2012, **189**(1), 49–54.
12 Y. Monakhova, *et al.*, New mixed lanthanum- and alkaline-earth cation-containing basic catalysts obtained by an alginate route, *Catal. Today*, 2012, **189**(1), 28–34.
13 F. Liu, *et al.*, Photoluminescent porous alginate hybrid materials containing lanthanide ions, *Biomacromolecules*, 2008, **9**(7), 1945–1950.
14 A. Haug and O. Smidsrød, Strontium–Calcium Selectivity of Alginates, *Nature*, 1967, **215**(5102), 757–757.
15 D. S. Morais, *et al.*, Biological evaluation of alginate-based hydrogels, with antimicrobial features by Ce(III) incorporation, as vehicles for a bone substitute, *J. Mater. Sci.: Mater. Med.*, 2013, **24**(9), 2145–2155.
16 A. Balint, *et al.*, *Synthesis of Nanoceria for Biomedical Applications*, in *International Conference on Advancements of Medicine and Health Care through Technology; 5th – 7th June 2014, Cluj-Napoca, Romania: MEDITECH 2014*, ed. S. Vlad and V. R. Ciupa, Springer International Publishing, Cham, 2014, pp. 317–320.
17 T. Sahu, *et al.*, Nanoceria: Synthesis and biomedical applications, *Curr. Nanosci.*, 2013, **9**(5), 588–593.
18 B. T. Stokke, *et al.*, Small-Angle X-ray Scattering and Rheological Characterization of Alginate Gels. 1. Ca−Alginate Gels, *Macromolecules*, 2000, **33**(5), 1853–1863.
19 P. Agulhon, *et al.*, Structural Regime Identification in Ionotropic Alginate Gels: Influence of the Cation Nature and Alginate Structure, *Biomacromolecules*, 2012, **13**(1), 215–220.
20 K. I. Draget, *et al.*, Small-Angle X-ray Scattering and Rheological Characterization of Alginate Gels. 3. Alginic Acid Gels, *Biomacromolecules*, 2003, **4**(6), 1661–1668.
21 O. Smidsrod, Properties of Poly(1,4-Hexuronates) in Gel State .2. Comparison of Gels of Different Chemical Composition, *Acta Chem. Scand.*, 1972, **26**(1), 79–88.
22 G. Skjakbraek, H. Grasdalen and O. Smidsrod, Inhomogeneous Polysaccharide Ionic Gels, *Carbohydr. Polym.*, 1989, **10**(1), 31–54.
23 A. Mikkelsen and A. Elgsaeter, Density distribution of calcium-induced alginate gels. A numerical study, *Biopolymers*, 1995, **36**(1), 17–41.
24 E. Schuster, *et al.*, Microstructural, mechanical and mass transport properties of isotropic and capillary alginate gels, *Soft Matter*, 2014, **10**(2), 357–366.
25 K. I. Draget, G. S. Braek and O. Smidsrod, Alginic Acid Gels - the Effect of Alginate Chemical-Composition and Molecular-Weight, *Carbohydr. Polym.*, 1994, **25**(1), 31–38.
26 A. Haug, O. Smidsrod and B. Larsen, Degradation of Alginates at Different pH Values, *Acta Chem. Scand.*, 1963, **17**(5), 1466–1468.
27 J. L. Major and T. J. Meade, Bioresponsive, Cell-Penetrating, and Multimeric MR Contrast Agents, *Acc. Chem. Res.*, 2009, **42**(7), 893–903.
28 M. Holz, S. R. Heil and A. Sacco, Temperature-dependent self-diffusion coefficients of water and six selected molecular

liquids for calibration in accurate 1H NMR PFG measurements, *Phys. Chem. Chem. Phys.*, 2000, **2**(20), 4740–4742.
29 E. O. Stejskal and J. E. Tanner, Spin Diffusion Measurements: Spin Echoes in the Presence of a Time-Dependent Field Gradient, *J. Chem. Phys.*, 1965, **42**(1), 288–292.
30 D. W. Schaefer and K. D. Keefer, Fractal Geometry of Silica Condensation Polymers, *Phys. Rev. Lett.*, 1984, **53**(14), 1383–1386.
31 D. Avnir, *et al.*, Is the Geometry of Nature Fractal?, *Science*, 1998, **279**(5347), 39–40.
32 B. P. Hills, C. Cano and P. S. Belton, Proton NMR relaxation studies of aqueous polysaccharide systems, *Macromolecules*, 1991, **24**(10), 2944–2950.
33 P. Kimberlee, C. T. Adrian and H. Laurence, Mapping of the spatial variation in alginate concentration in calcium alginate gels by magnetic resonance imaging(MRI), *Carbohydr. Res.*, 1993, **246**(1), 43–49.
34 N. E. Simpson, *et al.*, NMR properties of alginate microbeads, *Biomaterials*, 2003, **24**(27), 4941–4948.
35 D. Thom, *et al.*, Characterisation of cation binding and gelation of polyuronates by circular dichroism, *Carbohydr. Res.*, 1982, **100**(1), 29–42.
36 C. H. Yang, *et al.*, Strengthening Alginate/Polyacrylamide Hydrogels Using Various Multivalent Cations, *ACS Appl. Mater. Interfaces*, 2013, **5**(21), 10418–10422.